ORIGINAL ARTICLE



A single phosphorylatable amino acid residue is essential for the recognition of multiple potyviral HCPro effectors by potato Ny_{thr}

Bryce G. Alex¹ | Zong-Ying Zhang^{1,2} | Danny Lasky¹ | Hernan Garcia-Ruiz ©³ | Ronnie Dewberry¹ | Caitilyn Allen¹ | Dennis Halterman⁴ | Aurélie M. Rakotondrafara ©¹

²Ministry of Agriculture and Rural Affairs Key Laboratory of Pest Monitoring and Green Management, College of Plant Protection, China Agricultural University, Beijing, China

³Department of Plant Pathology and Nebraska Center for Virology, University of Nebraska-Lincoln, Lincoln, Nebraska,

⁴United States Department of Agriculture-Agricultural Research Service, Madison, Wisconsin, USA

Correspondence

Aurélie M. Rakotondrafara, Department of Plant Pathology, University of Wisconsin-Madison, Madison, WI, USA. Email: rakotondrafa@wisc.edu

Funding information

USDA-ARS-State Potato Cooperative Research, Grant/Award Number: MSN180673; Wisconsin Potato Industry Board, Grant/Award Number: MSN234734

Abstract

Potato virus Y (PVY, Potyviridae) is among the most important viral pathogens of potato. The potato resistance gene Ny_{thr} confers hypersensitive resistance to the ordinary strain of PVY (PVY^O), but not the necrotic strain (PVY^N). Here, we unveil that residue 247 of PVY helper component proteinase (HCPro) acts as a central player controlling Ny_{thr} strain-specific activation. We found that substituting the serine at 247 in the HCPro of PVY^O (HCPro^O) with an alanine as in PVY^N HCPro (HCPro^N) disrupts Ny_{thr} recognition. Conversely, an HCPro^N mutant carrying a serine at position 247 triggers defence. Moreover, we demonstrate that plant defences are induced against HCPro^O mutants with a phosphomimetic or another phosphorylatable residue at 247, but not with a phosphoablative residue, suggesting that phosphorylation could modulate Ny, the resistance. Extending beyond PVY, we establish that the same response elicited by the PVY^O HCPro is also induced by HCPro proteins from other members of the Potyviridae family that have a serine at position 247, but not by those with an alanine. Together, our results provide further insights in the strain-specific PVY resistance in potato and infer a broad-spectrum detection mechanism of plant potyvirus effectors contingent on a single amino acid residue.

KEYWORDS

callose, HCPro, hypersensitive resistance, Nytbr, potato virus Y, Potyviridae

INTRODUCTION

Plants have developed multiple layers of defence against viruses (Boualem et al., 2016). The first layer of innate defence against viruses is RNA silencing, which can target the viral genome for sequencespecific degradation. Many viruses disrupt this defence strategy by encoding suppressors of silencing (Nakahara & Masuta, 2014). The second layer of plant defence involves both pattern recognition

receptors (PRRs) and intracellular nucleotide-binding leucinerich repeat (NLR) immune receptors to detect pathogens (Jones & Dangl, 2006). PRRs typically recognize conserved microbial features or pathogen-associated molecular patterns (PAMPs), such as flagellin, chitin, or the double-stranded (ds)RNA formed during viral replication (Korner et al., 2013; Niehl et al., 2016) to induce a broad-spectrum pattern-triggered immunity (PTI) response. Plant NLRs recognize the presence of pathogen effector proteins inside

This is an open access article under the terms of the Creative Commons Attribution-NonCommercial-NoDerivs License, which permits use and distribution in any medium, provided the original work is properly cited, the use is non-commercial and no modifications or adaptations are made. © 2024 The Author(s). Molecular Plant Pathology published by British Society for Plant Pathology and John Wiley & Sons Ltd.

¹Department of Plant Pathology, University of Wisconsin-Madison, Madison, Wisconsin, USA

host cells to active effector-triggered immunity (ETI). PRR and NLR activation results in many of the same defence responses, including calcium flux, generation of reactive oxygen species (ROS), and cell wall reinforcement (Peng et al., 2018; Thulasi Devendrakumar et al., 2018; Tsuda & Katagiri, 2010). However, ETI generally culminates in a programmed cell death (PCD) at the site of infection to restrict the pathogen spread (Cui et al., 2015; Jones & Dangl, 2006).

In potato, hypersensitive resistance (HR) against the 9.7kb monopartite potyviral potato virus Y (PVY, Potyviridae family) is conferred by the N genes (Valkonen, 2015). HR following N gene activation induces PCD at the site of virus introduction, which is often accompanied by visible necrosis (Künstler et al., 2016). Resistance by most N genes is also strain-specific, with the Ny, Nc, and Nz genes conferring HR to strains PVYO, PVYC, and PVYZ, respectively (Valkonen, 2015). The limitation of these strain-specific resistances is well-illustrated by the potato cultivar Premier Russet (PR) (Novy et al., 2008), which contains an Ny_{thr} -like gene and is highly resistant to PVY^O but is susceptible to the necrotic and recombinant PVY^N strains. Ny targets the PVY multifunctional, viral-encoded helpercomponent proteinase (HCPro) protein (Moury et al., 2011; Tian & Valkonen, 2013), which is essential for aphid transmission, genome replication, movement, and suppression of RNA silencing (Valli et al., 2018).

Callose deposition is one of the earliest cellular responses after pathogen recognition and is thought to block or delay local and systemic movements of viruses through cell wall reinforcement and possibly by restricting plasmodesmal permeability (Amsbury et al., 2017; Chowdhury et al., 2020; Dobnik et al., 2013; Iglesias & Meins Jr., 2000). We previously established callose as a functional indicator of Ny_{tbr} resistance, observing significantly higher callose accumulation in Ny_{thr} PR plants inoculated with PVYO relative to those inoculated with PVYN:O, a strain with an O-type genome except for the N-type P1 and HCPro genes (Chowdhury et al., 2020). This strain-specific Ny_{tbr} recognition can be dissociated from viral replication. The transient expression of the HCPro effector from PVYO (HCProO) elicits a callose response in PR plants while the HCPro from the PVY^N (HCPro^N) does not (Chowdhury et al., 2020). PVY and its corresponding HCPro, independent of the strain, are capable of suppressing callose accumulation induced by flagellin 22 (flg22), a known bacterial elicitor and callose inducer (Gomez-Gomez & Boller, 2000), establishing HCPro function as a suppressor of PTI (Chowdhury et al., 2020). However, unlike the necrotic strain, PVY^O and its corresponding HCPro^O are unable to block flg22-induced callose accumulation in resistant PR potatoes (Chowdhury et al., 2020). The pathogenicity determinant was narrowed down to residues within the central domain of HCPro, which contains eight amino acid differences (N236I, L238K, A247S, I252V, R262Q, K269R, R270K and V301I) between HCPro^N and HCPro^O (Moury et al., 2011; Tian & Valkonen, 2013, 2015). The transient expression of a mutant version of HCPro^O, in which we introduced mutations encoding the eight amino acid changes in the N-type HCPro, escaped Ny_{thr} activation. Moreover, these mutations were sufficient to restore the ability of

HCPro^O to block flg22-induced callose despite the resistant genetic background of the plant, validating HCPro and the eight amino acid signature residues as the pathogen elicitor (Chowdhury et al., 2020).

Here, in the absence of an infectious clone, we used the HCPro transient expression system shown to mimic Nythr induction from full virus inoculation (Chowdhury et al., 2020) to test the effect of targeted HCPro changes on Ny_{thr} recognition. We identified a single amino acid within the delineated eight amino acid signature of HCPro at position 247, a serine residue in HCPro^O and an alanine residue in HCPro^N, as the central player of Ny_{thr} activation. Phosphorylation at this residue triggers callose accumulation while a mutation converting it into a phosphoablative amino acid effectively blocked any response. We analysed the natural variation of the eight amino acid signature residues of HCPro across 143 members of the Potyvirus genus within the Potyviridae family, the largest family of plant RNA viruses, and found the presence of a serine at position 247 in unrelated HCPro proteins sufficient to induce a resistance response by Ny_{thr} despite their low overall sequence identity to PVY HCPro^O. This work provides further insights in the strain-specific PVY resistance in potato and infers the functional fate of potyviral effectors dictated at a single amino acid level.

2 | RESULTS

2.1 | PVY infection facilitates *Ralstonia* solanacearum bacterial growth

We previously established that PVY infection can lead to suppression of PTI through the function of the HCPro effector (Chowdhury et al., 2020). This led us to assess whether such a suppression of the plant immune responses can predispose plants to other infection. We thus measured the growth rate of *R. solanacearum*, which causes bacterial wilt of potato, in PVY^O-infected potato cultivar Katahdin (Figure 1). Two weeks after viral inoculation, potato leaflets were infiltrated with virulent *R. solanacearum* GMI1000. Bacterial titres were determined in mock- and PVY-infected plants 0, 24 and 48 h post-inoculation (hpi) (Figure 1). The result shows a statistically significant difference in bacterial titre at least at 24 hpi, with higher *R. solanacearum* numbers in leaflets infected with PVY than in those mock-inoculated, in line with an increased susceptibility of PVY-infected plants to bacterial infection at least at the early stage of infection.

2.2 | A single amino acid substitution within HCPro is sufficient to induce Ny_{tbr} response

Previous studies established the significance of the eight amino acid polymorphisms (N236I, L238K, A247S, I252V, R262Q, K269R, R270K and V301I) between the central domain of PVY HCPro type N and type O for Ny_{thr} -mediated defence (Chowdhury et al., 2020;

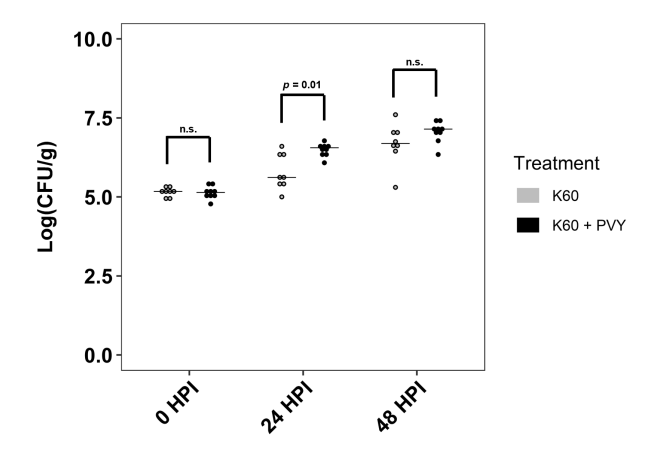


FIGURE 1 PVY infection facilitates *Ralstonia solanacearum* bacterial growth in Katahdin plants. Colony-forming units (cfu) were determined in plants 0, 24 and 48 h post-inoculation (hpi). The cfu values for each treatment and time point for both experimental repeats are represented individually (points) and with the median (line). Results from a t test (p < 0.05) of treatments at each timepoint is shown.

Tian & Valkonen, 2013). To determine whether these eight signature residues represent a conserved feature among other members of the Potyviridae family, we analysed the natural variations within these residues across 143 HCPro sequences available in NCBI (Figure S1). Note that the HCPro numbering used was proposed in Adams et al. (2005). The alignment revealed a striking conservation of an alanine (A) at position 247 (132 out of 143), as naturally found in PVYN HCPro, and relatively few (10 out of 143) with a serine (S) at the same position, as found in PVYO HCPro (Figure S1). This observation prompted us to investigate the functional relevance of the residue at position 247 in Ny_{thr} recognition. The nucleotides encoding a serine at position 247, called S247 for simplicity, in PVYO HCPro were changed to encode an alanine residue (HCPro^{O S247A}), mimicking that of PVYN HCPro. We used callose deposition read-out as a marker for the activation of plant defence responses in Ny_{thr}^{+} PR plants. The results showed that transient expression of HCPro^{O S247A} failed to trigger callose accumulation, akin to the wild-type HCPro^N (Figure 2a). Conversely, substitution of an alanine at the same position in PVYN HCPro with serine (HCProN A247S) shifted the HCProN strain-specific phenotype. It led to callose accumulation like that observed for the wild-type HCProO, in line with recognition by Nythr and activation of defence responses (Figure 2a).

We previously established that the PVY HCPro effector, independently of the strain, functions as a suppressor of PTI (Chowdhury et al., 2020). It hinders the induction of callose deposition by the synthetic 22 amino acid peptide from the conserved N-terminal part of flagellin (flg22), a known callose inducer (Gomez-Gomez & Boller, 2000). However, flg22-induced callose suppression by HCPro $^{\rm O}$ but not that of HCPro $^{\rm N}$ is compromised in $Ny_{tbr}^{\ \ +}$ PR plants (Chowdhury et al., 2020). We thus tested whether the single point mutations in HCPro $^{\rm O}$ S247A and HCPro $^{\rm N}$ A247S mutants would reverse the phenotype (Figure 2b). As previously established, infiltration of the PR potato leaflets with flg22 alone induced a callose response

(Figure 2b). The flg22-induced callose was significantly reduced in PR leaves expressing the HCPro O S247A mutant, but not in those expressing the HCPro N A247S mutant, relative to the empty Agrobacterium control (Figure 2b). This result mirrors phenotypes opposite to those of the wild-type sequences. When tested in PVY-susceptible Katahdin plants, neither of the HCPro variants triggered callose deposition due to the absence of Ny_{tbr} (Figure 2c). However, the HCPro O S247A mutant suppressed flg22-induced callose in Katahdin to a level comparable to the wild-type sequence (Figure 2d). This finding underscores the role of the single amino acid residue at position 247 in Ny_{tbr} activation but not in its ability to suppress PTI. The retention of the flg22-induced callose suppression function by the HCPro O S247A mutant in Katahdin plants indicated that the amino acid substitution did not affect the overall protein stability.

To further rule out inherent differences in expression between HCPro variants in planta, we evaluated relative HCPro transcript abundance using reverse transcription-quantitative PCR (RT-qPCR). The results showed similar expression levels across the four HCPro variants (Figure S2). Protein accumulation was then assessed using green fluorescent protein (GFP)-tagged HCPro^O and HCPro^{O S247A}. The expression of the GFP-tagged HCPro^O in PR plants produced similar callose response phenotypes with the untagged protein (Figure S3a,b). We next compared the protein accumulation of the GFP-tagged HCPro^O and HCPro^{O S247A} proteins in both Katahdin and PR potato leaves using crude extracts. HCPro^O and HCProO^{S247A} proteins accumulated to similar level at the expected size of c. 75 kDa in both cultivars (Figure S3c). It is worth noting the presence of an additional band at c. 50 kDa. This analysis confirmed that both protein variants showed similar stability in both potato cultivars.

2.3 | Phosphorylation status of HCPro residue 247 could modulate Ny_{thr} recognition

The relevance of the serine residue in Ny_{thr} activation prompted us to explore whether phosphorylation of S247 plays a modulatory role in HCPro^O recognition. We first used in-silico methods to predict the likelihood of phosphorylation occurring at S247 (Figure S4). The predictive tools assigned a high score to S247 phosphorylation, and the kinase-specific and motif prediction methods indicated that S247 resides within a conserved putative kinase substrate motif RKLSIG (Figure S4). Next, we substituted the S247 in HCPro^O for an aspartic acid (HCPro^{O S247D}), a modification that functionally mimics a phosphorylated residue due to the covalently attached negative charge. Additionally, we introduced mutations to change the serine residue to another phosphorylatable amino acid, threonine (HCPro^{O S247T}). We compared the callose response of these mutants to that of the phosphoablated HCPro^{O S247A} mutant and of the wild-type sequence in Ny_{thr} PR plants (Figure 3a,b) and in susceptible Katahdin plants (Figure 3c,d). The results showed that both the phosphomimetic HCPro^{O S247D} and the phosphorylatable HCPro^{O S247T} mutants retained the $\mathrm{HCPro}^{\mathrm{O}}$ strain-specific phenotype in Ny_{tbr}^{+} plants, evident through increased callose accumulation (Figure 3a) and their

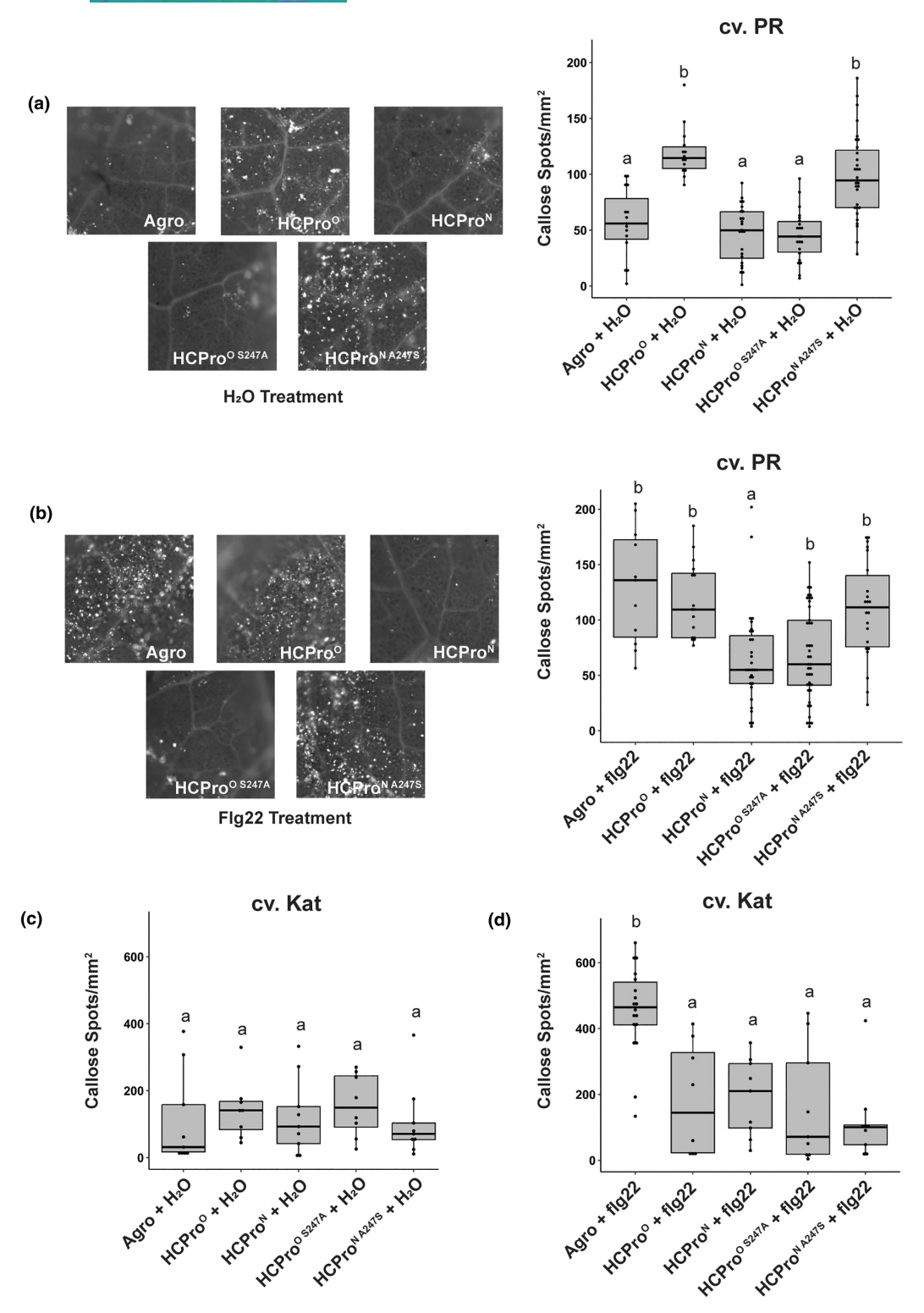


FIGURE 2 Effect of HCPro amino acid 247 on callose accumulation. Representative images of callose deposition responses and callose counts/mm² following transient expression of the indicated proteins following water or flg22 treatment. Callose counts/mm² are shown from expressions of HCPro^O and HCPro^N mutants in (a) Premier Russet (PR) plants ($n \ge 14$); (b) PR plants with flg22 ($n \ge 11$); (c) Katahdin (Kat) plants ($n \ge 8$); and (d) Kat plants with flg22 ($n \ge 8$). Kruskal–Wallis test ($\alpha < 0.05$) was used to test for statistical significance. Means marked with the same letter are not statistically different according to Dunn's test (p < 0.05). The cultivar is indicated above each plot.

failure to suppress flg-22 induced callose (Figure 3b). These results contrasted with the phosphoablated HCPro^{O S247A} mutant, which failed to trigger callose accumulation (Figure 3a) and maintained

its ability to suppress flg22-induced callose (Figure 3b) in PR plants. In susceptible Katahdin plants, all HCPro variants, including HCPro^{O S247D}, HCPro^{O S247T} and HCPro^{O S247A}, failed to trigger any

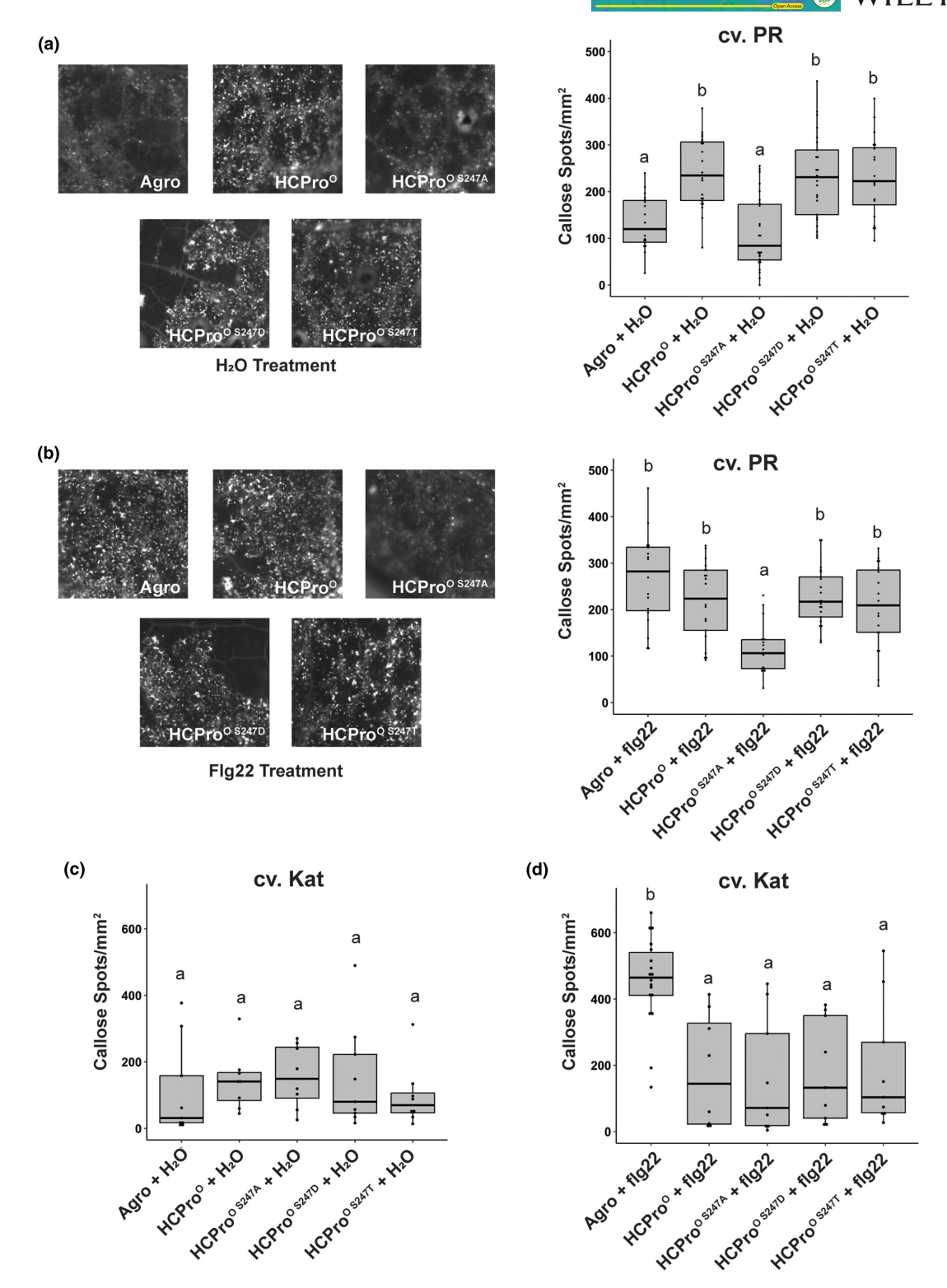


FIGURE 3 Effect of phosphomimetic and phosphoablative substitutions at site 247 in HCPro on callose accumulation. Representative images of callose deposition responses and callose counts/mm² following transient expression of the indicated proteins following water or flg22 treatment. Callose counts/mm² are shown from expression of HCPro^O mutants in (a) Premier Russet (PR) plants ($n \ge 18$); (b) PR plants with flg22 ($n \ge 19$); (c) Katahdin (Kat) plants ($n \ge 8$); and (d) Kat plants with flg22 ($n \ge 8$). Kruskal–Wallis test (a < 0.05) was used to test for statistical significance. Means marked with the same letter are not statistically different according to Dunn's test (p < 0.05). The cultivar is indicated above each plot.

callose accumulation (Figure 3c), consistent with the lack of Ny_{tbr} . Additionally, they all effectively suppressed flg22-induced callose, like the wild-type HCPro $^{\circ}$ in the Katahdin plants (Figure 3d).

2.4 | Response to the phosphomimetic and wild-type HCPro^O is lost at elevated temperature

We previously demonstrated that an increase in temperature from 20 to 28°C compromised Ny_{thr}-mediated resistance, resulting in a failure to induce callose deposition upon PVYO infection or transient expression of HCPro^O (Chowdhury et al., 2020). We tested whether phosphorylation at S247 could still trigger defence when Ny_{thr}-mediated resistance is impaired. We examined callose accumulation in PR plants in response to transient expression of the phosphomimetic HCPro O S247D at elevated growth temperature. Following infiltration with HCPro, PR plants were either kept at 20°C or placed at 28°C for 24 h. We included the wild-type HCPro^O and HCPro^N as controls. The results obtained from plants kept at 20°C were consistent with earlier findings, with increased callose accumulation for HCProO and HCProO S247D relative to empty Agrobacterium control and HCProN, as expected for the induction of resistance by these two HCPro proteins (Figure 4a). In contrast, when plants were subjected to 28°C, irrespective of the resistance genetic background, no significant differences in callose accumulation were observed among the HCPro variants. This suggests that the phosphorylated state of HCPro alone is insufficient to trigger defence when Nythr resistance is compromised (Figure 4a). We next examined the HCPro ability to suppress flg22-induced callose at elevated temperature. At 20°C. only HCPro^N reduced callose accumulation to a level similar to the empty Agrobacterium control. However, at 28°C, all HCPro variants, including the phosphomimic HCPro^O, reduced flg22-induced callose down to control level. The restoration of flg22-induced callose suppression activity at 28°C suggests that expression of the HCPro variants was not impaired at high temperatures and provides further evidence that Ny_{tbr} induction disrupts this activity for HCPro^O and HCPro^{O S247D}.

2.5 | Ny_{tbr} recognizes S247 within diverse potyviral HCPro proteins

Our earlier analysis of the natural variations within the eight amino acid signature distinguishing HCPro^N and HCPro^O across 143 HCPro sequences available in NCBI uncovered that 10 potyviral HCPro sequences bear a serine residue at position 247 (Figure S1). Their phylogenetic reconstruction reveals that these potyviruses with a serine at this specific site were distributed across six distinct clades whose basal lineages have an alanine (Figure 5). Further sequence analysis showed that the S247 in all 10 HCPro sequences are within a conserved putative kinase substrate motif RKLSIG as we observed in PVYO HCPro (Figures S4 and S5).

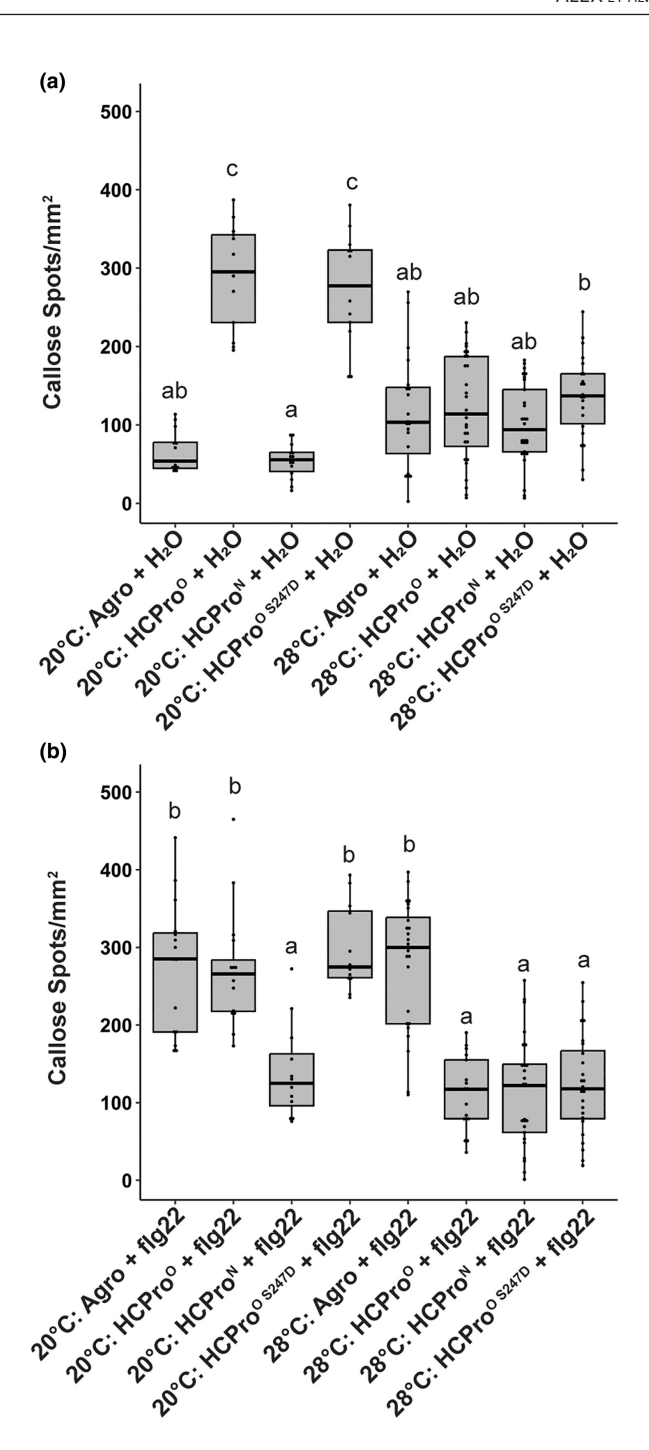


FIGURE 4 Callose accumulation of the wild type and phosphomimetic mutant HCPro $^{\rm O}$ is lost at 28°C. Representative images of callose deposition responses and callose counts/mm $^{\rm 2}$ following transient expression of the indicated proteins following water or flg22 treatment. Callose counts/mm $^{\rm 2}$ are shown from HCPro expression in (a) Premier Russet (PR) plants kept at 20°C and at 28°C ($n \ge 13$); and (b) PR plants kept at 20°C and at 28°C with flg22 ($n \ge 12$). Kruskal–Wallis test ($\alpha < 0.05$) was used to test for statistical significance. Means marked with the same letter are not statistically different according to Dunn's test (p < 0.05).

The correlation between the nature of the residue at position 247 and Ny_{tbr} resistance led us to explore whether the presence of S247 in those potyviral HCPro proteins could trigger Ny_{tbr} -mediated

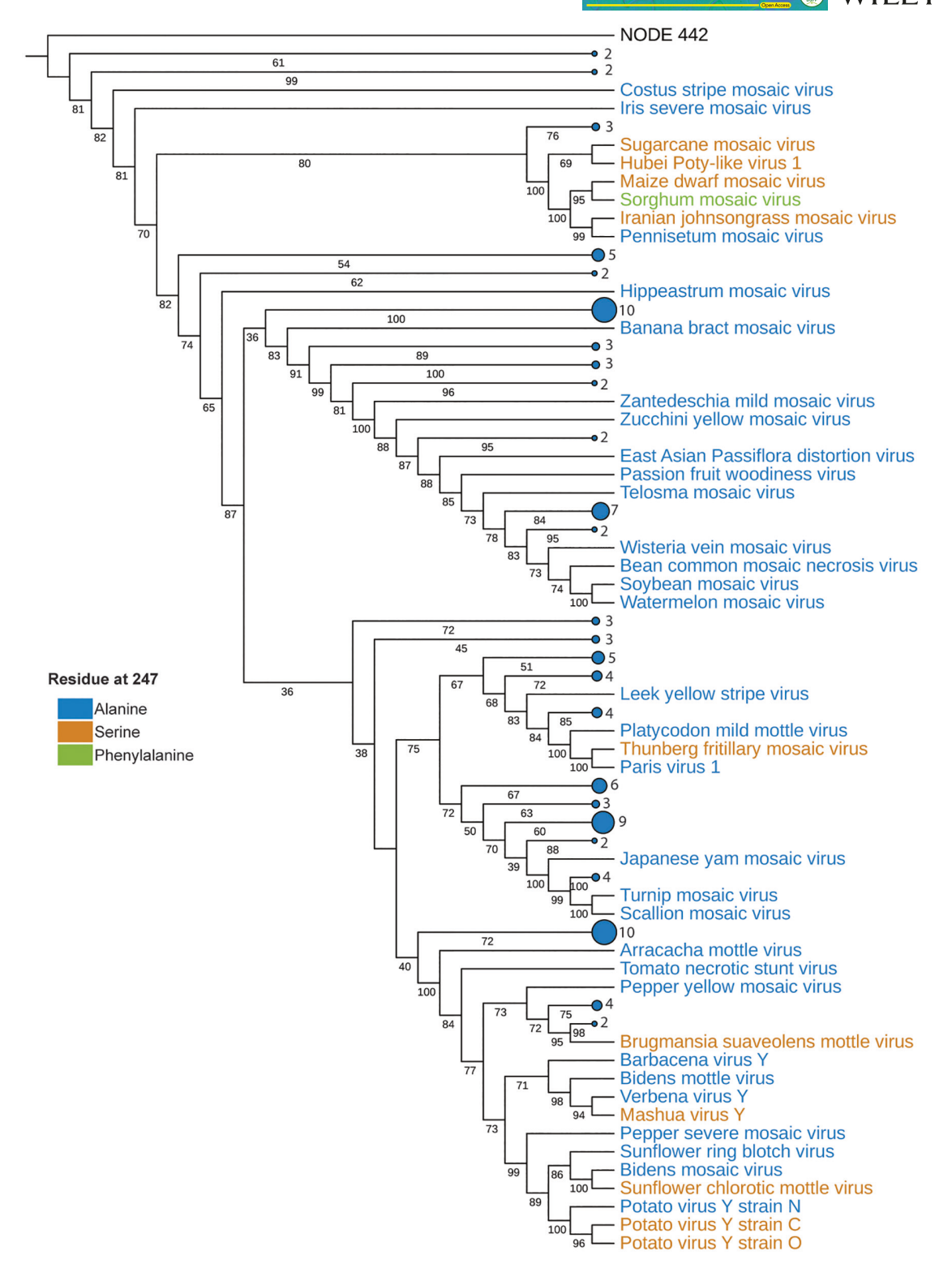


FIGURE 5 Diversity of HCPro amino acid 247. Maximum-likelihood tree of the RDRP amino acid sequences from 143 potyviruses (Table S5). Numbers below the nodes represent ultrafast bootstrap (UFBoot) values (Minh et al., 2013), where UFBoot ≥95 is considered strong support. Clades that did not include viruses tested for defence induction and that only contained members with an alanine aligned to the PVY HCPro site 247 were collapsed. Sample size is given next to these nodes. Leaf label colour was assigned according to the residue aligned to HCPro 247.

defence. We first tested two PVY-unrelated HCPro sequences with overall low sequence identity, one with an alanine residue (*Turnip mosaic virus* [TuMV] HCPro) and the other with a serine (*Sugarcane mosaic virus* [SCMV] HCPro) at position 247, for their responses

in PR plants. When we transiently expressed SCMV HCPro in the PR plants, it led to callose accumulation like that of PVY^O HCPro (Figure 6a). In contrast, the expression of TuMV HCPro that bears an alanine at position 247 failed to induce callose accumulation above

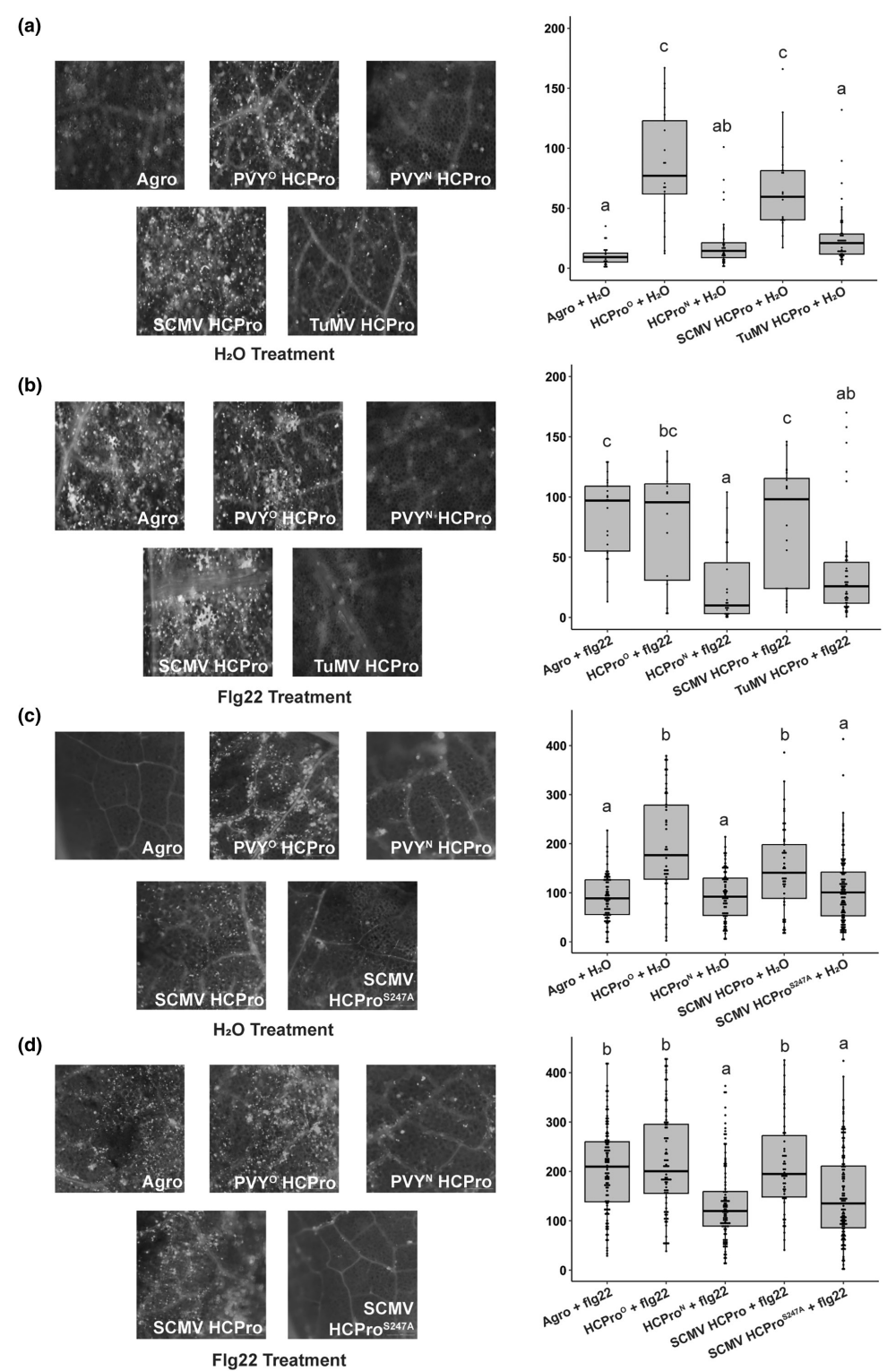


FIGURE 6 HCPro site 247 in diverse potyviruses determines Ny_{tbr} recognition. Representative images of callose deposition responses and callose counts/mm² following transient expression of the indicated proteins following water or flg22 treatment. Callose counts/mm² are shown from PVY, TuMV and SCMV HCPro expressions in (a) Premier Russet (PR) plants ($n \ge 20$); (b) PR plants with flg22 ($n \ge 15$). Callose counts/mm² are also shown for the mutant SCMV HCPro^{5247A} in (c) PR plants ($n \ge 45$); (d) PR plants with flg22 ($n \ge 50$). Kruskal–Wallis test ($\alpha < 0.05$) was used to test for statistical significance. Means marked with the same letter are not statistically different according to Dunn's test (p < 0.05).

HCPro^N or the empty *Agrobacterium* control (Figure 6a). When we tested their ability to suppress flg22-induced callose in the PR plants, TuMV HCPro showed callose suppressor activity, limiting

flg22-induced callose accumulation to a similar level to PVY^N HCPro (Figure 6b). In contrast, SCMV HCPro failed to suppress flg22-induced callose accumulation (Figure 6b).

To substantiate that the single amino acid at position 247 was a central player in recognition by Ny_{tbr} , we substituted the nucleotides encoding S247 in the SCMV HCPro with those for an alanine residue (SCMV HCPro 5247A). This single amino-acid change resulted in a significant reduction in callose accumulation in PR plants, consistent with an evasion of Ny_{tbr} recognition (Figure 6c). This loss of recognition correlated with the recovery of the flg22-callose deposition suppression function (Figure 6d).

To further isolate HCPro 247 residue as the determinant of Ny the avirulence, independently of the virus natural host range and surrounding sequences, we expanded the assay to additional HCPro proteins including that of Brugmansia suaveolens mottle virus (BsMoV), Pepper mottle virus (PepMoV), Sorghum mosaic virus (SrMV), Soybean mosaic virus (SMV), and Sunflower chlorotic mottle virus (SCMoV). These have generally low degrees of amino acid sequence similarity to PVYO HCPro (Table 1) but bear either a serine or an alanine at position 247. It is worth noting that SrMV bears a nonphosphorylatable phenylalanine residue at that position. Our result confirmed the functional significance of the residue at position 247 in Ny_{the} recognition. PepMoV and SMV, which bear an alanine at 247, as well as SrMV that naturally bears a phenylalanine at that position, exhibited significantly reduced callose accumulation relative to the PVYO HCPro (Figure S6, Table 2). In contrast, the HCPro proteins harbouring a serine at 247 (BsMoV and SCMoV) heightened callose accumulation (Figure S6, Table 2).

2.6 | HCPro proteins from diverse potyviruses exhibit structural similarity in the region functionally linked to Ny_{thr} induction

The low amino acid sequence identity of HCPro proteins that trigger Ny_{thr} defence (Table 1) prompted us to investigate whether

structural similarity surrounding S247 might be consistent with a shared functional role. We produced a structural alignment of HCPro 3D models generated by AlphaFold2 (Jumper et al., 2021). The results revealed structural similarity across the HCPro proteins from potyviruses that induced a resistance response in PR (Figure 7a). The structural resemblance extended to the region between amino acids 227 to 327 encompassing the PVY HCPro signature amino acids at position 236, 238, 247, 252, 262, 269, 270 and 301 (Figure 7b). For the SCMV, BsMoV and SCMoV models, the proportion of the total number of modelled residues that were structurally equivalent to the PVYO HCPro model fell between 95% and 97% (Table S2). Structural similarity in this region is consistent with a shared mechanism of Ny_{tbr} defence induction by the HCPro proteins with S247.

2.7 | HCPro suppression of callose is independent of its primary function in RNA silencing

One of the primary functions of potyviral HCPro proteins in promoting infection is their ability to suppress host RNA silencing (Valli et al., 2018). We analysed whether the HCPro function in suppressing PTI is dependent on its silencing suppressor function. We first compared the silencing suppression activity of the PVY^O and PVY^N HCPro proteins, and a previously established mutant HCPro^O in which the eight amino acid signature residues were swapped with those of HCPro^N (HCPro^M) that expresses HCPro^N strain-specific phenotype (Chowdhury et al., 2020), using a standard transient green fluorescent protein (GFP) transgene silencing in wild-type *Nicotiana benthamiana* (Figure 8a) (Johansen & Carrington, 2001). We measured the ability of HCPro^O, HCPro^N, and HCPro^M to suppress RNA silencing and subsequently lead to GFP accumulation. The silencing activity of the different HCPro variants were tested

TABLE 1 Sequence identity of potyviral HCPro proteins compared to the PVY^O HCPro and conservation among potyviruses at sites within the HCPro signature motif distinguishing the PVY^O from PVY^N strain groups.

Potyvirus species	Identity with PVY ^O HCPro (%)	Alignment to PVY signature region
PVY ^O	100	irkhpngtrklsignlvpldlaefrommkgoyrkopgvskkotsskognvypcccttlodgsav
PVY^N	92	nrlhengtrklaignliveldlaefrr mkgoykroegvskkotsskognyvyeccottlefgkpa
SCMV	41	trfnengorkisigkiv pldfokiresfvglp nrop gkcovski ggy lypcccvit sgdpv
TuMV	48	TRAVPNGSRKLAIGKLIVPTNFEVLREQMKG PEPYPV VEG SKLQGDEVHACCCVTTDDGSAV
BsMoV	63	irknengerklsignlivpldlmefrk mcg dtnoplvgkog smkdsne vpcccvtrddgop
PepMoV	64	drtiengsrklaignliveldlaefrk mngidtooppe gkyctsoldgnfvyecccttlddgtav
SCMoV	77	IRVHPNGARKLSIGNLIVPLDLAEFROMMKG F KOPTVGKOCTSLK GNFVYPCCCTTLDDGKAF
SMV	46	vrknengorelaisslivpldferarmalogks/trgpl/macisrodgnfvypcccvth-fgopv
SrMV	38	trfnengorkifirkiv pldfokirdsfvgio okoalskac rki nny ceeccvtt

Note: The amino acid sequence-based percentage identity shared with the PVY^O HCPro is shown for the HCPro proteins from PVY^N, SCMV, TuMV, BsMoV, PepMoV, SCMoV, SMV and SrMV. The amino acid residues aligning to the PVY^N HCPro residues 236-301, or the PVY strain-specific signature region (Chowdhury et al., 2020, Tian & Valkonen, 2013), are also shown for each HCPro protein sequence. The position corresponding to the PVY^N HCPro site 247 is indicated with a star. Each position in the alignment is shaded black if it is present in at least four of the seven total sequences, grey if the residue is chemically similar to the consensus residue, and white otherwise.

Potyvirus species	Residue at 247	Comparison to PVY ^N HCPro (<i>p</i> -value)	Comparison to PVY ^O HCPro (p-value)
BsMoV	S	<0.001	0.93
SCMoV	S	0.005	0.64
PepMoV	Α	0.11	0.008
SMV	Α	0.2	0.009
SrMV	F	0.44	0.008

TABLE 2 Summary of callose phenotype following transient expression in PR plants of the HCPro proteins from BsMoV, SCMoV, PepMoV, SMV, and SrMV compared to the PVY^N and PVY^O HCPro proteins.

Note: The p-value from a Mann–Whitney U test of callose counts/mm² compared to the PVY^N HCPro and PVY^O HCPro is reported.

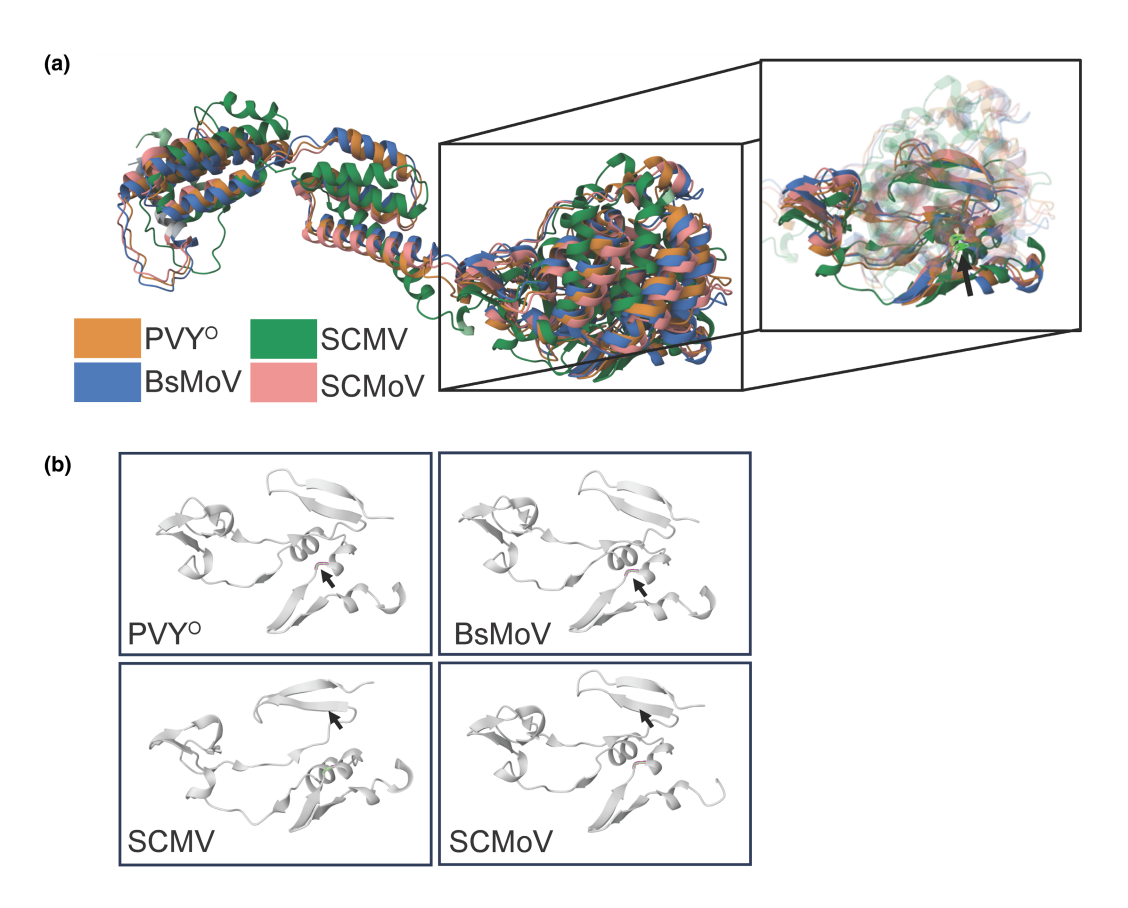
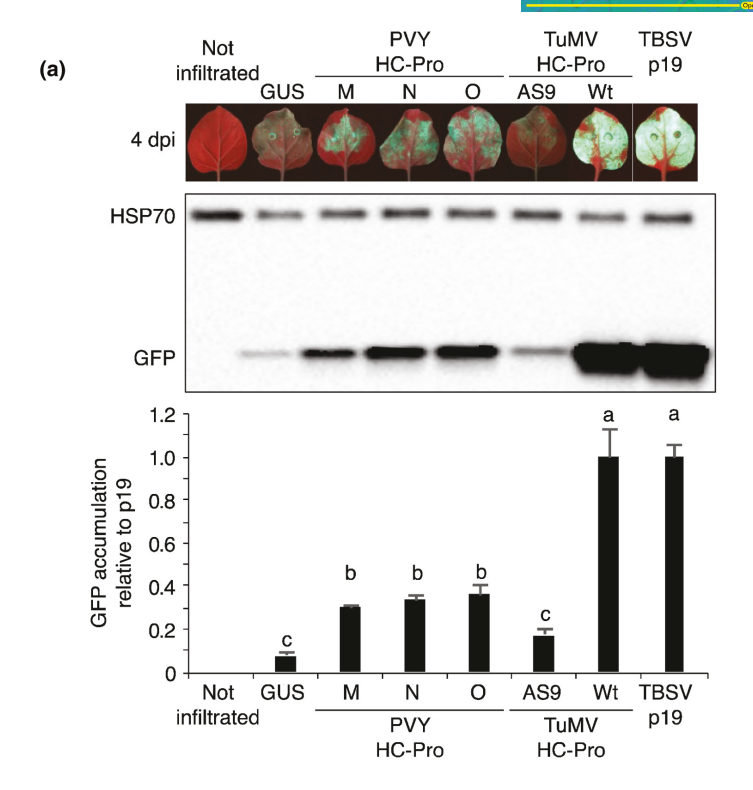


FIGURE 7 Structural conservation of HCPro proteins that induced Ny_{tbr}^+ defence. (a) Structural alignment of the HCPro proteins from PVY^O, BsMoV, SCMV, and SCMoV. Each model was given a unique colour, and the regions of the BsMoV, SCMV, and SCMoV HCPro models that match the reference structure (PVY^O HCPro) are in full colour, while unaligned regions are lighter. The regions highlighted correspond to residues 236, 238, 247, 252, 262, 269, 270, and 301 that define the signature region distinguishing PVY^O from PVY^N and that are within the central domain of HCPro, which encompasses residue 100–311. (b) The structure of the region encompassing amino acids 227–327 that includes the PVY signature residues from each virus are depicted individually. In both (a) and (b), the serine from each potyviral HCPro protein that aligns with the PVY^O HCPro S247 is highlighted and indicated with an arrow.

in parallel with well-characterized silencing suppressors, including *Tomato bushy stunt virus* (TBSV) P19 protein, HCPro from TuMV and the silencing suppression-deficient mutant TuMV HCPro AS9 (Garcia-Ruiz et al., 2010). Leaves were co-infiltrated with the construct expressing GFP and the silencing suppressor, and the GFP fluorescence in the leaves was visualized by UV light and GFP accumulation was quantified at day 4 post-infiltration, relative to that the heat shock protein 70 (HSP70) internal control (Figure 8a). In wild-type *N. benthamiana*, transient GFP expression was naturally

silenced (Johansen & Carrington, 2001). The co-infiltration assay confirmed that the PVY HCPro variants were active in transgene silencing suppression and increased GFP expression as shown in the protein blot (Figure 8a).

To assess the suppression of silencing function of HCPro in relation to its suppression of PTI function, we performed a callose assay of the silencing deficient TuMV HCPro AS9 mutant. Our result revealed that for the TuMV HCPro AS9 mutant, which has lost its ability to suppress RNA silencing (Figure 8a), callose accumulation



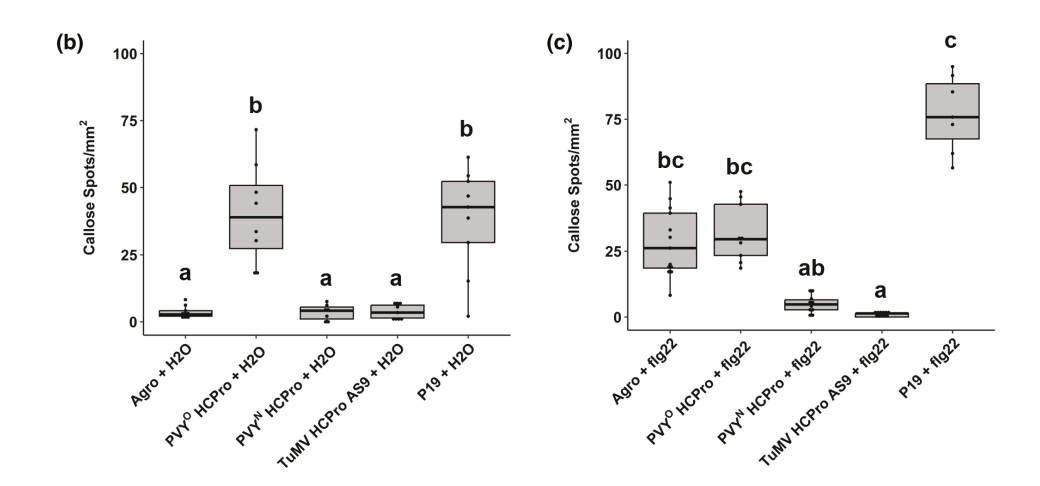


FIGURE 8 Flg22-induced callose accumulation in the presence of a TuMV silencing-deficient HCPro mutant. (a) RNA silencing suppression of HCPro $^{\rm O}$, HCPro $^{\rm N}$, and HCPro $^{\rm M}$ (Chowdhury et al., 2020), relative to that of the TuMV HCPro, suppression-deficient TuMV HCPro AS9 mutant, and the TBSV P19 in *Nicotiana benthamiana*. Clones were evaluated using a standard transient GFP transgene silencing. Pictures show GFP fluorescence at 4 days after co-infiltration of GFP with the indicated protein. Non-infiltrated plants, plants infiltrated with unrelated β -glucuronidase (GUS) protein, and the suppression-deficient HCPro AS9 from TuMV were used as negative controls. The wild-type TuMV HCPro and TBSV P19 were used as positive controls. HSP70 was used as loading control for the representative western blot showing GFP accumulation. The histogram shows the average accumulation \pm SE of four biological replicates. Significance was evaluated with a one-way analysis of variance followed by Tukey-Kramer's post hoc analysis. Bars with the same letter are not statistically different (Tukey's test, α =0.01). (Callose accumulation in the PVY $^{\rm O}$ -resistant Premier Russet cultivar following PVY $^{\rm O}$ HCPro, TuMV silencing-deficient HCPro AS9 mutant, and TBSV P19 transient expression following water (n \geq 7) (b) or flg22 (n \geq 7) (c) treatment. Kruskal-Wallis test (α <0.05) was used to test for statistical significance. Means marked with the same letter are not statistically different according to Dunn's test (p<0.05).

did not differ significantly from that observed for the PVY HCPro^N and the empty Agrobacterium control (Figure 8b), consistent with the absence of Ny_{thr} induction. However, flg22-induced callose

accumulation was significantly reduced in the presence of the mutant compared to the empty *Agrobacterium* control (Figure 8c), in line with non-overlapping functions.

3 | DISCUSSION

In this study, we provide an example of the functional fate of a viral effector dictated at a single amino acid level. We use our previous observation that transient expression of the PVY^O HCPro protein is sufficient to induce strain-specific Ny_{tbr} resistance (Chowdhury et al., 2020) to show that the strain specificity of Ny_{tbr} recognition is due to one single amino acid difference between PVY^O and PVY^N at HCPro position 247. Our results hint that Ny_{tbr} activation may be dependent on the phosphorylation state of the amino acid. Furthermore, our findings extend beyond PVY. We demonstrated that defences within the Ny_{tbr}^+ PR cultivar can be triggered by HCPro proteins from other potyviruses with a serine at 247, an amino acid composition mirroring that of PVY^O HCPro.

The conservation of the HCPro site 247 at the amino acid and structural levels suggests that it is important for HCPro function. The independent alanine to serine substitutions that have occurred at 247 throughout potyviral evolution could also mean that these functional differences are adaptative under different circumstances. However, it is unclear what the underlying function or adaptive significance might be. HCPro is a multifunctional protein with an Nterminal region that contains a putative insect vector binding site, and a central region that contains RNA-binding domains with a role in silencing (Valli et al., 2018). The C-terminal region encodes a viral capsid binding region for movement and a protease domain. Residue 247 is positioned immediately upstream of the Important in Genome amplification (IGN) motif, which is associated with virus movement and amplification (Cronin et al., 1995), and is downstream of positions 244 and 245, which are associated with suppression of RNA silencing and enhancement of viral particle yield (Valli et al., 2018). The proximity of site 247 to several functional sites could act as a guide for a more detailed analysis of the molecular mechanisms involved in Ny_{thr} recognition. While residue 247 is situated between the functionally linked motifs used to distinguish the central region from the N- and C-terminal regions of HCPro (Valli et al., 2018), improved structural prediction methods can be used to further refine boundaries of structurally and functionally distinct regions of HCPro.

Our results also laid the groundwork for future experiments with potyviral infectious clones to inform its role in other steps of viral infection and fitness. Additionally, while we were able to validate expression of our HCPro constructs at the transcriptional (Figure S2) and translational (Figure S3) levels, and by monitoring the effects of the HCPro variants on the plant callose phenotype, further work is needed to clarify how differences in expression and protein properties among HCPro variants contribute to the observed callose phenotypes.

While the exact role of S247 in pathogenicity remains unclear, our results uncover a general model for Ny_{tbr} resistance activation where the phosphorylation state of that residue may play a central role. The lack of defence response with the phosphomimic HCPro $^{\rm O~S247D}$ mutant at elevated temperature suggests that phosphorylation of HCPro alone is not sufficient to trigger defence unless Ny_{tbr} signalling is intact. The substitution with a phosphoablative residue (S247A) abolished the defence response, while the phosphomimic residues

(S247D, S247T) maintained HCPro recognition. Despite a generally low degree of amino acid sequence similarity to PVY^O HCPro, a similar response was observed with the unrelated SCMV HCPro, which bears a phosphorylatable residue at position 247. The phosphorylation prediction tools revealed that S247 is a target for modification and is within a consensus RKLSIG that could act as a substrate for basophilic kinases in all 10 HCPro protein sequences that bear a serine at that position. Furthermore, the single swap of the alanine with a serine in PVY^N HCPro and in the other alanine-bearing HCPros reconstituted the consensus phosphokinase motif from the native RKLAIG sequence motif and resulted in callose accumulation.

Previous studies predicted that the eight amino acid residues that differ between HCPro $^{\rm O}$ and HCPro $^{\rm N}$ may be responsible for changing the HCPro protein structure to render PVY $^{\rm N}$ avirulent in potato with Ny_{tbr} resistance (Tian & Valkonen, 2013, 2015). While our analysis using Alphafold prediction failed to see any broad structural differences between the HCPro proteins from PVY $^{\rm O}$ and PVY $^{\rm N}$, there was a striking similarity in the S247 structural environment across diverse potyviruses. This structural similarity may explain the observed functional similarity in the presence of Ny_{tbr} among potyviral HCPro proteins that share low amino acid sequence identity.

Our observation that PVY infection may favour bacterial growth supports its function in suppression of PTI. Plant viruses have been largely considered non-PAMP-encoding pathogens (Huang, 2021), but recent work has shown that PTI is active against both viruses (Korner et al., 2013) and dsRNA (Niehl et al., 2016), and that viral movement proteins (MP) are capable of suppressing dsRNA-induced PTI (Huang et al., 2023). The suppression of PAMP-triggered immune responses has also been demonstrated for other viral proteins, including the *Plum pox virus* coat protein (PPV CP) (Nicaise & Candresse, 2017), *Cauliflower mosaic virus* P6 (Zvereva et al., 2016), and the *Cucumber mosaic virus* movement protein (Kong et al., 2018). Our findings offer an insight on the strain-specific responses mediated by HCPro, which is independent of its primary function as a suppressor of RNA silencing.

Despite the fact that the phyllosphere can support dense populations of microbes, we are only beginning to understand the interplay between multiple plant pathogens during co-infection. The observation that the widely spread PVY in potato production can favour *R. solanacearum* infection, which is the world's second most damaging bacterial plant pathogen, undermines the ecological role of viruses as potential drivers of evolution of disease epidemics and severity.

4 | EXPERIMENTAL PROCEDURES

4.1 | Plant material and growth conditions

Potato cultivars Premier Russet (PR) (Novy et al., 2008), which contains an Ny_{tbr} -like gene, and Katahdin, which lacks any resistance against potato virus Y (Nie et al., 2012) were propagated and maintained in a greenhouse under 12-h light/dark, and daytime/

night-time temperatures of 22/17°C. Three-week-old plants were used for all experiments.

Nicotiana benthamiana plants were maintained in the growth chamber at 22°C with 16 h-light/8 h dark cycle. The plants had six to eight leaves at the time of infiltration.

4.2 | Ralstonia solanacearum strain K60 accumulation assay

Two-week-old Katahdin plants were rub-inoculated with frozen N. benthamiana leaves infected with PVY $^{\rm O}$ (accession number NY090031) ground in 0.2M KHPO $_4$ inoculation buffer. Mock-inoculated plants were rub inoculated with buffer only. Infection was confirmed using PVY immunostrips (Agdia). Two weeks post-inoculation, 2×10^5 cfu/mL of R. solanacearum K60 were infiltrated into plant leaves. Plants were then kept at 90% humidity. Bacterial numbers were derived as the cfu in a leaf tissue sample taken with a no. 3 cork borer (9 mm diameter) at 0, 24 and 48 h post-infiltration. The experiment was performed twice with at least three replicates each.

4.3 | Plasmids and mutagenesis

The nucleotide sequences coding for the full HCPro from PVYO (GenBank: JX424837, amino acids 299-740), PVYN (GenBank: X97895, amino acids 276-740), and the mutant PVYO (HCProM) with the eight amino acid substitutions (N236I, L238K, A2247S, I252V, R262Q, K269R, R270K, and V301I), were synthesized by Twist Bioscience, cloned into the pTwist ENTR vector adapted for use with Gateway cloning technology (Thermo Fisher), and recombined into the Gateway-compatible binary vector pGWB2 (Nakagawa et al., 2007) under control of the Cauliflower mosaic virus 35S promoter for expression using Agrobacterium tumefaciens GV3101, as previously described (Chowdhury et al., 2020). The nucleotide sequences used for cloning can be found in Table S1. The same was done for the HCPro from other potyviruses; their GenBank accession and range are provided in Table S3. The TuMV HCPro, the TuMV AS9 mutant HCPro, the SCMV HCPro, and TBSV P19 were as described in Garcia-Ruiz et al. (2010) and Bacheller (2017).

The HCPro mutants at position 247 were generated with PCR using the QuickChange site-directed mutagenesis strategy (Agilent) with the above PVY^O HCPro or PVY^N HCPro cassette in the pTwist ENTR vector as a template. The primers used for mutagenesis are provided in Table S4. PCR amplification was performed with PfuUltra II fusion High-fidelity DNA polymerase (Agilent) and the product was treated with DpnI (NEB) to remove the original template. Finally, the product was directly transformed into competent Escherichia coli DH5 α (NEB).

To generate the GFP-tagged HCPro proteins, the sequences for HCPro^O and HCPro^{O S247A} were translationally fused to N-terminal GFP driven by a CaMV 35S promoter in the binary expression construct pSH42 through ligation-independent cloning (LIc).

4.4 | Agroinfiltration

Glycerol stocks of strain GV3101 of A. *tumefaciens* stored at -80° C were streaked onto Luria Bertani (LB) agar and left at room temperature (RT) for 3 days before infiltration. Single colonies were selected for overnight growth at RT in 10 mL LB broth with the appropriate antibiotics. Bacteria were then collected by centrifugation at 3200g for 5 min, washed in pH 5.5 MMA buffer without the acetosyringone (10 mM MgCl₂, 10 mM (*N*-morpholino) ethanesulfonic acid [MES]), and centrifuged again. The bacterial pellet was resuspended in MMA with 200 μ M acetosyringone and brought to an OD₆₀₀ of 0.8 (0.5 for agroinfiltration of *N. benthamiana*). Finally, the bacterial solution was incubated at RT for 2 h, then pressure infiltrated into the abaxial surfaces of the leaves (Abdullah & Halterman, 2018).

4.5 | Callose assay

After 24h following agroinfiltration, leaves were syringe infiltrated with either water or $1\,\mu\text{M}$ synthetic flg22 peptide (GenScript USA Inc.). At 48 hpi, punches were taken from infiltrated leaflets using a no. 3 cork borer (7.5 mm diameter) and placed in $200\,\mu\text{L}$ of destaining solution (1:3 acetic acid: ethanol) in a 96-well plate. The 96-well plate was rotated on an orbital shaker at 150 rpm overnight at RT. Following overnight incubation in the destaining solution, the destaining solution was replaced by $200\,\mu\text{L}$ of $67\,\text{mM}$ K₂HPO₄ (pH12) and incubated for 2h. The wash solution was then replaced with $200\,\mu\text{L}$ of $67\,\text{mM}$ K₂HPO₄ (pH12) with 0.01% (wt/vol) aniline blue (Sigma -Aldrich) and incubated overnight.

Prior to imaging, the $\rm K_2HPO_4$ and aniline blue solution was replaced with 50 μ L of 50% glycerol. Punches were imaged using the BioTek Cytation 7 Cell Imaging Multimode Reader and the Gen5 software (v. 3.13) at 10× resolution with the DAPI filter (excitation wavelength 377 nm, emission wavelength 447 nm). Callose quantification followed the approach as detailed in Mason et al. (2020). The Trainable Weka Segmentation (TWS) plug-in (https://imagej.net/Trainable_Weka_Segmentation) was then used to identify and quantify callose deposits.

For the assay of the flg22-induced callose deposition suppression function of HCPro at elevated temperatures, plants were infiltrated as described above. After 24h at 20°C, two sets of plants were placed at either 20 or 28°C for another 24h. The plant leaflets were then treated with water or $1\mu M$ of flg22 and left at their respective temperatures for 24h. Leaf punches were then harvested, stained, and imaged as described above.

In every experiment, each condition was randomly assigned to at least two leaflets. Between two and six punches were taken from each leaflet, and between two and six different microscopic fields of each leaf disc were imaged. Each experiment was independently repeated at least twice. The boxplots and dot plots shown are callose counts/mm² from the experimental replicates. The minimum number of replicates for a condition is indicated for each of the depicted experiments.

4.6 | RT-qPCR

At 48h post-agroinfiltration, total RNA was extracted from six Katahdin leavesperconstructtested (emptyvector, HCPro $^{\rm O}$, HCPro $^{\rm N}$, HCPro $^{\rm OS247A}$, HCPro $^{\rm N}$ using the RNeasy Plant Mini Kit (Qiagen). Complementary DNA (cDNA) was then synthesized using an iScript cDNA Synthesis Kit (Bio-Rad) per the manufacturer's instructions. The expression level of HCPro was evaluated using RT-qPCR with primers targeting shared HCPro sequences (Forward: 5'-GTGCCAAAGCTTGGAACCTG-3', Reverse: 5'-TTCTAGGCAGTTCTGCATCAT-3'). Reactions were performed in a 10- μ L volume with the SsoAdvanced Universal SYBR Green Supermix (Bio-Rad) in a C1000 Touch PCR thermal cycler (Bio-Rad) under the following conditions: 95°C for 3min, then 39 cycles of 95°C for 10s and 57°C for 30s.

4.7 | Protein extraction and western blot

Agrobacteria were prepared for agroinfiltration according to the protocol detailed above, and syringe infiltrated into the leaves of Premier Russet and Katahdin potato plants. After 3 days, proteins were extracted in a buffer containing 50 mM Tris-HCl (pH7.5), 150 mM NaCl, 0.2% Triton X-100, 10% (vol/vol) glycerol, and protease inhibitor mixture (Sigma-Aldrich). The crude protein extracts were then separated on a 4%–20% gradient gel (Bio-Rad), and the protein blots were stained with Ponceau S and next probed with an anti-GFP antibody (Merck Millipore).

4.8 | Transient suppression of RNA silencing assay

The suppressor of silencing function of PVY HCPro variants was tested using the standard green-fluorescent protein (GFP) transgene silencing in wild-type *N. benthamiana* by co-infiltration (Johansen & Carrington, 2001). β-glucuronidase (GUS) and suppression-deficient TuMV AS9 HCPro mutants were used as a negative control. The wild-type TuMV HCPro and TBSV P19 were used as positive controls (Garcia-Ruiz et al., 2010). Suppression of silencing was assessed by the intensity of the green fluorescence 4 days after co-infiltration of GFP plasmid with the indicated proteins. The GFP and the HSP70 accumulation was visualized by protein blot using anti-GFP (Merck Millipore) and anti-HSP70 (Merck Millipore) antibodies, respectively.

4.9 | Statistical analysis

Statistical analyses were performed using the R software (R Core Team, 2018). Data was checked for normality using the Shapiro-Wilk test and through Q-Q plot visualization. Homogeneity of variances was tested using Levene's test. Normally distributed data with homogeneous variances were evaluated for significance using a

one-way analysis of variance (ANOVA) followed by Tukey's honestly significant difference. Data that were non-normally distributed or had non-homogeneous variances were evaluated for significance using the Kruskal–Wallis test unless otherwise indicated. Dunn's test following Bonferroni *p*-value adjustment was used for multiple comparisons. Callose staining data from leaflets infiltrated with water or flg22 were analysed separately.

4.10 | Sequence alignment and phylogenetics

The alignments and phylogenetic analysis included 143 sequences from viruses in *Potyviridae* available in NCBI. GenBank accession numbers included are provided in Table S5. HCPro and RNA-dependent RNA polymerase (RDRP) sequences were treated separately. Sequences were first aligned with Clustal Omega (Sievers & Higgins, 2018) with default parameters. Sequence logos were generated using WebLogo3 (Crooks et al., 2004). A maximum-likelihood tree was generated from the RDRP sequence alignment using W-IQ-TREE (Trifinopoulos et al., 2016) with the ModelFinder (Kalyaanamoorthy et al., 2017) and UFBoot (Minh et al., 2013) options enabled. The RDRP sequence from a member of the *Protopotyvirus* clade (GenBank JAAOEH010000445.1) described in Wolf et al. (2020) was used as an outgroup for a total of 144 RDRP sequences in the RDRP tree.

4.11 | In silico phosphorylation prediction and structural modelling

NetPhos v. 3.1 (Blom et al., 1999), PhosphoSVM (Dou et al., 2014), and MusiteDeep (Wang et al., 2020) were used to determine the likelihood of phosphorylation at a given site, and NetPhos v. 3.1, Eukaryotic Linear Motif (ELM) (Kumar et al., 2022), and Scansite v. 4.0 (Obenauer et al., 2003) were used to identify sequence motifs that could act as substrates for particular kinase groups.

Models of HCPro were generated with AlphaFold2 (Jumper et al., 2021) using MMseqs2 (Steinegger & Soding, 2017) via ColabFold (Mirdita et al., 2022) (v. 1.5.2). Model quality from each method was evaluated with global quality score metrics assembled with the Protein Structure Validation Suite (Bhattacharya et al., 2007) (v. 1.5). Residue exposure was determined with DeepREx-WS (Manfredi et al., 2021). The jFATCAT algorithm with the rigid option was used to generate structural alignments (Prlic et al., 2010).

ACKNOWLEDGEMENTS

The study was funded by Wisconsin Potato Industry Board (MSN234734) to A.M.R. and USDA-ARS-State Potato Cooperative Research (MSN180673) to A.M.R. and D.H. The funders had no role in study design, data collection and interpretation or the decision to submit the work for publication.

DATA AVAILABILITY STATEMENT

The data that support the findings of this study are available on request from the corresponding author.

ORCID

Hernan Garcia-Ruiz https://orcid.org/0000-0002-4681-470X Aurélie M. Rakotondrafara https://orcid.org/0000-0002-1859-3743

REFERENCES

- Abdullah, S. & Halterman, D. (2018) Methods for transient gene expression in wild relatives of potato. *Methods in Molecular Biology*, 1848, 131–138.
- Adams, M.J., Antoniw, J.F. & Beaudoin, F. (2005) Overview and analysis of the polyprotein cleavage sites in the family *Potyviridae*. *Molecular Plant Pathology*, 6, 471–487.
- Amsbury, S., Kirk, P. & Benitez-Alfonso, Y. (2017) Emerging models on the regulation of intercellular transport by plasmodesmata-associated callose. *Journal of Experimental Botany*, 69, 105–115.
- Bacheller, N.E. (2017) Detecting, cloning, and screening for suppressors of RNA silencing in maize chlorotic mottle virus and sugarcane mosaic virus [PhD dissertation]. Lincoln, NE: University of Nebraska-Lincoln.
- Bhattacharya, A., Tejero, R. & Montelione, G.T. (2007) Evaluating protein structures determined by structural genomics consortia. *Proteins*, 66. 778–795.
- Blom, N., Gammeltoft, S. & Brunak, S. (1999) Sequence and structurebased prediction of eukaryotic protein phosphorylation sites. *Journal of Molecular Biology*, 294, 1351–1362.
- Boualem, A., Dogimont, C. & Bendahmane, A. (2016) The battle for survival between viruses and their host plants. *Current Opinion in Virology*, 17, 32–38.
- Chowdhury, R.N., Lasky, D., Karki, H., Zhang, Z., Goyer, A., Halterman, D. et al. (2020) HCPro suppression of callose deposition contributes to strain-specific resistance against potato virus Y. *Phytopathology*, 110, 164–173.
- Cronin, S., Verchot, J., Haldeman-Cahill, R., Schaad, M. C. & Carrington, J. C. (1995). Long-distance movement factor: a transport function of the potyvirus helper component proteinase. *The Plant Cell*, 7, 549–559.
- Crooks, G.E., Hon, G., Chandonia, J.M. & Brenner, S.E. (2004) WebLogo: a sequence logo generator. *Genome Research*, 14, 1188–1190.
- Cui, H., Tsuda, K. & Parker, J.E. (2015) Effector-triggered immunity: from pathogen perception to robust defense. *Annual Review of Plant Biology*, 66, 487–511.
- Dobnik, D., Baebler, S., Kogovsek, P., Pompe-Novak, M., Stebih, D., Panter, G. et al. (2013) β -1,3-glucanase class III promotes spread of PVY^{NTN} and improves in planta protein production. *Plant Biotechnology Reports*, 7, 547–555.
- Dou, Y., Yao, B. & Zhang, C. (2014) PhosphoSVM: prediction of phosphorylation sites by integrating various protein sequence attributes with a support vector machine. *Amino Acids*, 46, 1459–1469.
- Garcia-Ruiz, H., Takeda, A., Chapman, E.J., Sullivan, C.M., Fahlgren, N., Brempelis, K.J. et al. (2010) Arabidopsis RNA-dependent RNA polymerases and dicer-like proteins in antiviral defense and small interfering RNA biogenesis during turnip mosaic virus infection. The Plant Cell, 22, 481–496.
- Gomez-Gomez, L. & Boller, T. (2000) FLS2: an LRR receptor-like kinase involved in the perception of the bacterial elicitor flagellin in Arabidopsis. Molecular Cell, 5, 1003–1011.
- Huang, C. (2021) From player to pawn: viral avirulence factors involved in plant immunity. *Viruses*, 13, 688.

- Huang, C., Sede, A.R., Elvira-Gonzalez, L., Yan, Y., Rodriguez, M.E., Mutterer, J. et al. (2023) dsRNA-induced immunity targets plasmodesmata and is suppressed by viral movement proteins. *The Plant Cell*, 35, 3845–3869.
- Iglesias, V.A. & Meins, F., Jr. (2000) Movement of plant viruses is delayed in a β -1,3-glucanase-deficient mutant showing a reduced plasmodesmatal size exclusion limit and enhanced callose deposition. *The Plant Journal*, 21, 157–166.
- Johansen, L.K. & Carrington, J.C. (2001) Silencing on the spot. Induction and suppression of RNA silencing in the *Agrobacterium*-mediated transient expression system. *Plant Physiology*, 126, 930–938.
- Jones, J.D.G. & Dangl, J.L. (2006) The plant immune system. *Nature*, 444, 323–329.
- Jumper, J., Evans, R., Pritzel, A., Green, T., Figurnov, M., Ronneberger, O. et al. (2021) Highly accurate protein structure prediction with AlphaFold. *Nature*, 596, 583–589.
- Kalyaanamoorthy, S., Minh, B.Q., Wong, T.K.F., von Haeseler, A. & Jermiin, L.S. (2017) ModelFinder: fast model selection for accurate phylogenetic estimates. *Nature Methods*, 14, 587–589.
- Kong, J., Wei, M., Li, G., Lei, R., Qiu, Y., Wang, C. et al. (2018) The cucumber mosaic virus movement protein suppresses PAMP-triggered immune responses in *Arabidopsis* and tobacco. *Biochemical and Biophysical Research Communications*, 498, 395–401.
- Korner, C.J., Klauser, D., Niehl, A., Dominguez-Ferreras, A., Chinchilla, D., Boller, T. et al. (2013) The immunity regulator BAK1 contributes to resistance against diverse RNA viruses. *Molecular Plant-Microbe Interactions*, 26, 1271–1280.
- Kumar, M., Michael, S., Alvarado-Valverde, J., Meszaros, B., Samano-Sanchez, H., Zeke, A. et al. (2022) The eukaryotic linear motif resource: 2022 release. *Nucleic Acids Research*, 50, D497–D508.
- Künstler, A., Bacsó, R., Gullner, G., Hafez, Y.M. & Király, L. (2016) Staying alive—is cell death dispensable for plant disease resistance during the hypersensitive response? *Physiological and Molecular Plant Pathology*, 93, 75–84.
- Manfredi, M., Savojardo, C., Martelli, P.L. & Casadio, R. (2021) DeepREx-WS: a web server for characterising protein-solvent interaction starting from sequence. Computational and Structural Biotechnology Journal, 19, 5791–5799.
- Mason, K.N., Ekanayake, G. & Heese, A. (2020) Staining and automated image quantification of callose in *Arabidopsis* cotyledons and leaves. *Methods in Cell Biology*, 160, 181–199.
- Minh, B.Q., Nguyen, M.A. & von Haeseler, A. (2013) Ultrafast approximation for phylogenetic bootstrap. Molecular Biology and Evolution, 30, 1188–1195.
- Mirdita, M., Schutze, K., Moriwaki, Y., Heo, L., Ovchinnikov, S. & Steinegger, M. (2022) ColabFold: making protein folding accessible to all. *Nature Methods*, 19, 679–682.
- Moury, B., Caromel, B., Johansen, E., Simon, V., Chauvin, L., Jacquot, E. et al. (2011) The helper component proteinase cistron of potato virus Y induces hypersensitivity and resistance in potato genotypes carrying dominant resistance genes on chromosome IV. *Molecular Plant–Microbe Interactions*, 24, 787–797.
- Nakagawa, T., Kurose, T., Hino, T., Tanaka, K., Kawamukai, M., Niwa, Y. et al. (2007) Development of series of Gateway binary vectors, pGWBs, for realizing efficient construction of fusion genes for plant transformation. *Journal of Bioscience and Bioengineering*, 104, 34–41.
- Nakahara, K.S. & Masuta, C. (2014) Interaction between viral RNA silencing suppressors and host factors in plant immunity. Current Opinion in Plant Biology, 20, 88–95.
- Nicaise, V. & Candresse, T. (2017) Plum pox virus capsid protein suppresses plant pathogen-associated molecular pattern (PAMP)triggered immunity. *Molecular Plant Pathology*, 18, 878–886.
- Nie, B., Singh, M., Murphy, A., Sullivan, A., Xie, C. & Nie, X. (2012) Response of potato cultivars to five isolates belonging to four strains of potato virus Y. Plant Disease, 96, 1422–1429.

- Niehl, A., Wyrsch, I., Boller, T. & Heinlein, M. (2016) Double-stranded RNAs induce a pattern-triggered immune signaling pathway in plants. *New Phytologist*, 211, 1008–1019.
- Novy, R.G., Whitworth, J.L., Stark, J.C., Love, S.L., Corsini, D.L., Pavek, J.J. et al. (2008) Premier Russet: a dual-purpose, potato cultivar with significant resistance to low temperature sweetening during long-term storage. *American Journal of Potato Research*, 85, 198–209.
- Obenauer, J.C., Cantley, L.C. & Yaffe, M.B. (2003) Scansite 2.0: proteomewide prediction of cell signaling interactions using short sequence motifs. *Nucleic Acids Research*, 31, 3635–3641.
- Peng, Y., van Wersch, R. & Zhang, Y. (2018) Convergent and divergent signaling in PAMP-triggered immunity and effector-triggered immunity. *Molecular Plant–Microbe Interactions*, 31, 403–409.
- Prlic, A., Bliven, S., Rose, P.W., Bluhm, W.F., Bizon, C., Godzik, A. et al. (2010) Pre-calculated protein structure alignments at the RCSB PDB website. *Bioinformatics*, 26, 2983–2985.
- R Core Team. (2018) R: a language and environment for statistical computing. Vienna, Austria: R Foundation for Statistical Computing. https://www.R-project.org/ [Accessed 15th October 2024]
- Sievers, F. & Higgins, D.G. (2018) Clustal omega for making accurate alignments of many protein sequences. Protein Science, 27, 135–145.
- Steinegger, M. & Soding, J. (2017) MMseqs2 enables sensitive protein sequence searching for the analysis of massive data sets. *Nature Biotechnology*, 35, 1026–1028.
- Thulasi Devendrakumar, K., Li, X. & Zhang, Y. (2018) MAP kinase signalling: interplays between plant PAMP- and effector-triggered immunity. *Cellular and Molecular Life Sciences*, 75, 2981–2989.
- Tian, Y.P. & Valkonen, J.P.T. (2013) Genetic determinants of potato virus Y required to overcome or trigger hypersensitive resistance to PVY strain group O controlled by the gene Ny in potato. *Molecular Plant-Microbe Interactions*, 26, 297–305.
- Tian, Y.P. & Valkonen, J.P.T. (2015) Recombination of strain O segments to HCpro-encoding sequence of strain N of potato virus Y modulates necrosis induced in tobacco and in potatoes carrying resistance genes Ny or Nc. Molecular Plant Pathology, 16, 735–747.
- Trifinopoulos, J., Nguyen, L.T., von Haeseler, A. & Minh, B.Q. (2016) W-IQ-TREE: a fast online phylogenetic tool for maximum likelihood analysis. *Nucleic Acids Research*, 44, W232–W235.

- Tsuda, K. & Katagiri, F. (2010) Comparing signaling mechanisms engaged in pattern-triggered and effector-triggered immunity. *Current Opinion in Plant Biology*, 13, 459–465.
- Valkonen, J.P. (2015) Elucidation of virus-host interactions to enhance resistance breeding for control of virus diseases in potato. *Breeding Science*. 65, 69–76.
- Valli, A.A., Gallo, A., Rodamilans, B., Lopez-Moya, J.J. & Garcia, J.A. (2018) The HCPro from the *Potyviridae* family: an enviable multitasking helper component that every virus would like to have. Molecular Plant Pathology, 19, 744–763.
- Wang, D., Liu, D., Yuchi, J., He, F., Jiang, Y., Cai, S. et al. (2020) MusiteDeep: a deep-learning based webserver for protein posttranslational modification site prediction and visualization. *Nucleic Acids Research*, 48, W140-W146.
- Wolf, Y.I., Silas, S., Wang, Y., Wu, S., Bocek, M., Kazlauskas, D. et al. (2020) Doubling of the known set of RNA viruses by metagenomic analysis of an aquatic virome. *Nature Microbiology*, 5, 1262–1270.
- Zvereva, A.S., Golyaev, V., Turco, S., Gubaeva, E.G., Rajeswaran, R., Schepetilnikov, M.V. et al. (2016) Viral protein suppresses oxidative burst and salicylic acid-dependent autophagy and facilitates bacterial growth on virus-infected plants. *New Phytologist*, 211, 1020–1034.

SUPPORTING INFORMATION

Additional supporting information can be found online in the Supporting Information section at the end of this article.

How to cite this article: Alex, B.G., Zhang, Z.-Y., Lasky, D., Garcia-Ruiz, H., Dewberry, R., Allen, C. et al. (2024) A single phosphorylatable amino acid residue is essential for the recognition of multiple potyviral HCPro effectors by potato Ny_{tbr}. Molecular Plant Pathology, 25, e70027. Available from: https://doi.org/10.1111/mpp.70027